ChemPhysChem

Research Article
doi.org/10.1002/cphc.202400072

Chemistry Europe
European Chemical Societies Publishing

www.chemphyschem.org

Accurate Experimental Structure of 1-Chloronaphthalene

Pablo Pinacho,*[a, b] Pablo Gómez,[a] Juan Carlos López,[a] and Susana Blanco*[a]

The structure of isolated 1-chloronaphthalene has been investigated in a supersonic expansion by high-resolution chirped-pulse Fourier transform microwave (CP-FTMW) spectroscopy in the 2–8 GHz frequency range. Accurate values of the rotational, centrifugal distortion, and nuclear quadrupole coupling constants for the only availabe conformer have been determined. The intensity of the spectrum allowed us to observe all the heavy atoms isotopologues in natural abundance, determining their rotational constants. From the extensive experimental dataset we derived accurate structures for 1-chloronaphthalene using different methodologies and compared with related compounds.

Introduction

Polycyclic aromatic hydrocarbons (PAHs) are ubiquitous molecules, crucial for humankind for their important applications in diverse fields; for their astrochemical implications, but also for their environmental hazard and toxicity.[1,2] Naphthalene ($C_{10}H_8$) is the smallest molecule which can be considered a PAH and thus, it constitutes a good model to start the study of their structures and intramolecular interactions.[3] The substitution of hydrogen atoms in naphthalene with chlorine atoms (from one to eight) gives rise to a new family of compounds, polychlorinated naphthalenes (PCNs). Chlorine alters to a large extent the physical and chemical properties of naphthalene, together with deforming its structure. In naphthalene the C–C bond lengths can be explained attending to the number of resonance forms present (Figure S1). By the mesomeric and inductive effects of chlorine,[4] new resonance structures appear, distorting the C–C bonds and angles. On one hand it extracts electronic charge from the aromatic ring (−I) since chlorine is more electronegative than carbon. On the other hand, the lone pairs of chlorine can participate in the resonance, donating electronic charge into the ring (+M).

The presence of PCNs in the environment, and the exposure to them is a topic of increasing interest due to its toxicity and carcinogenic effects.[5,6] These compounds are nowadays considered as mayor organic pollutants to be controlled and reduced.[7] PCNs were widely used in the industry for many years because of their stability, flame resistance and antiviral and antifungal properties. In the last decades there has been a decrease in the production and emission of PCNs, and currently the mayor source is the unintentional formation in industry processes.[5] Apart from their emission, PCNs can also be formed directly in the atmosphere by the reaction of naphthalene and free chlorine radical, following a photochemical mechanism.[7,8]

Among the PCNs, one of the most important is 1-chloronaphthalene (1-Cl-Naph, Figure 1). It is produced by the direct chlorination of naphthalene, and until the 1970s it was a common solvent widely used. As other PCNs, 1-Cl-Naph can be formed in the atmosphere by the photochemical reaction of naphthalene and radical chlorine species. This mechanism could even happen in the interstellar medium (ISM), due to the energetic conditions in some regions.[9] Recently, 1- and 2-cyanonaphthalene have been discovered in the ISM.[10] This fact, together with the confirmed presence in the ISM of several neutral and radical species containing chlorine,[11] make 1-Cl-Naph a promising candidate molecule to be detected in the ISM.

Due to the relevance of 1-Cl-Naph for its search in the ISM, for its atmospheric reactivity, or its applications in industry,[11–13] it is interesting to accurately determine its structure in an isolated environment. Rotational spectroscopy is a powerful technique to determine molecular structures based on the rotational fingerprints of the molecules in a supersonic expansion. The other mono-chlorinated isomer, 2-Cl-naphthalene (2-Cl-Naph), has been investigated much more in detail, including its phosphorescence emission spectrum,[14] its electronic spectrum in a molecular beam,[15] or its rotationally resolved fluorescence excitation spectrum.[16] For the latter, a

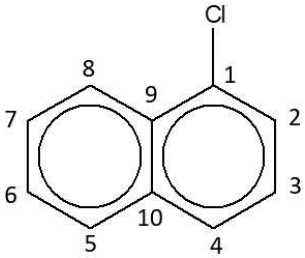

Figure 1. Schematic representation of 1-chloronaphthalene (1-Cl-Naph).

[a] P. Pinacho, P. Gómez, J. C. López, S. Blanco
Department of Physical Chemistry and Inorganic Chemistry, IU-CINQUIMA
University of Valladolid, Paseo Belen 7, Valladolid, 47011 Spain
E-mail: pablo.pinacho@ehu.eus
susana.blanco@uva.es

[b] P. Pinacho
Department of Physical Chemistry, University of the Basque Country (UPV/EHU), B° Sarriena, S/N, Leioa, 48940, Spain

Supporting information for this article is available on the WWW under https://doi.org/10.1002/cphc.202400072

high-resolution study, provides accurate values of the rotational constants, centrifugal distortion constants, and the nuclear quadrupole coupling constants for the ground state of 2-Cl-Naph, together with interesting properties of the excited states.

The band contours of 2-Cl-Naph, 1-Cl-Naph and its fluorinated analogue, 1-F-naphpthalene, were recorded and analyzed with vapor-phase electronic absorption spectroscopy.[17,18] In this work, the rotational constants of 1-Cl-Naph in the ground state were estimated.[17] The structure of 1-Cl-Naph has been described by X-ray diffraction,[19] however, it has not been investigated in depth using high-resolution rotational spectroscopy.

We had three goals when we started this work. The first one was to derive an accurate experimental structure for 1-Cl-Naph and compare with similar compounds to obtain information about the extension of the inductive and mesomeric effects of chlorine. The second was to provide a complete dataset for the search of 1-ClNaph in the ISM. Finally, we aimed to set the basis for future studies of 1-Cl-Naph microsolvation.

Experimental and Theoretical Methods

The spectrum was recorded in the chirped-pulse Fourier transform microwave (CP-FTMW)[20] spectrometer coupled with supersonic expansion at the University of Valladolid.[21,22] The sample of 1-Cl-Naph, a colorless liquid, was heated to approximately 120 °C in a stainless steel heated reservoir close to the pulsed nozzle. The vapors of the sample were mixed with argon as carrier gas at relative backing pressure of 2 bar. The molecule was introduced in the vacuum chamber by a supersonic expansion pulse of 900 μs length through a 1 mm nozzle. After the supersonic expansion, the electromagnetic radiation in the microwave region was generated by an arbitrary waveform generator, amplified by a 20 W solid-state amplifier, and transmitted into the vacuum chamber by a horn antenna. The radiation interacted with the isolated molecules in the supersonic expansion and induced a macroscopic polarization of the ensemble. Once the radiation pulse ceased, the molecular emission signal was recorded as the free induction decay in the time domain. The spectrum was converted to the frequency domain by the application of a fast Fourier transform. The spectrometer worked in a fast-frame set-up, with 8 excitation-emission cycle per each supersonic expansion. The repetition rate of the supersonic expansion was 5 Hz, giving a total of 40 repetitions per second. A total of 2.3 M averages were collected for the final spectrum of 1-Cl-Naph. To complete the 2–8 GHz spectrum three recording steps of 2 GHz each were conducted. The spectrometer features an uncertainty in frequency measurement better than 15 kHz, and a resolution power better than 25 kHz, enough to resolve the hyperfine structure arising from the nuclear quadrupole coupling of the ^{35}Cl and ^{37}Cl nuclei.

No conformational search was carried out for 1-Cl-Naph, as it is a completely rigid molecule, with only one conformation (Figure 1). The geometry of the molecule was optimized at the B3LYP-D3(BJ)/6-311++G(2d,p) level of theory,[23,24] including Grimme's dispersion correction[25] and Becke-Johnson damping function (D3(BJ)),[26] followed by re-optimization at MP2/6-311++G(2d,p).[27] The calculations were performed using Gaussian 16 revision A.03.[28]

Results and Discussion

Assignment of the Rotational Spectrum

The spectrum of 1-Cl-Naph features intense transitions. The typical pattern of lines with a relative intensity ratio 3:1 was observed and attributed to the rotational transitions arising from 1-^{35}Cl-Naph and 1-^{37}Cl-Naph. Due to the non-spherical distribution of nuclear charge in both nuclei, each rotational transition is split in several components, which appear as a hyperfine structure in the experimental spectrum (Figure 2). The fit of the experimental parameters and its assignment to the only conformation of 1-Cl-Naph was straightforward. A preliminary fit was performed using the JB95 software,[29] while the final measurements and fit were achieved by using the S-reduced semirigid rotor Hamiltonian in the I^r representation[30,31] using Pickett's CALPGM suite of programs[32] together with the AABS package.[33] The rotational constants, centrifugal distortion constants and quadrupole coupling constants for 1-^{35}Cl-Naph and 1-^{37}Cl-Naph are presented in Table 1.

The signal-to-noise ratio in the 1-Cl-Naph spectrum was sufficient for the observation of all the monosubstituted heavy atom isotopologues. We observed intense lines arising from the molecule with the ^{37}Cl nucleus with *ca.* 1/3 the intensity of the parent spectrum. The spectra arising from the ^{13}C monosubstituted isotopomers in natural abundance (1.1 %) were also fitted (Table S1). The experimental frequencies observed for all the species are collected at the end of the supplementary information (Tables S5–S7).

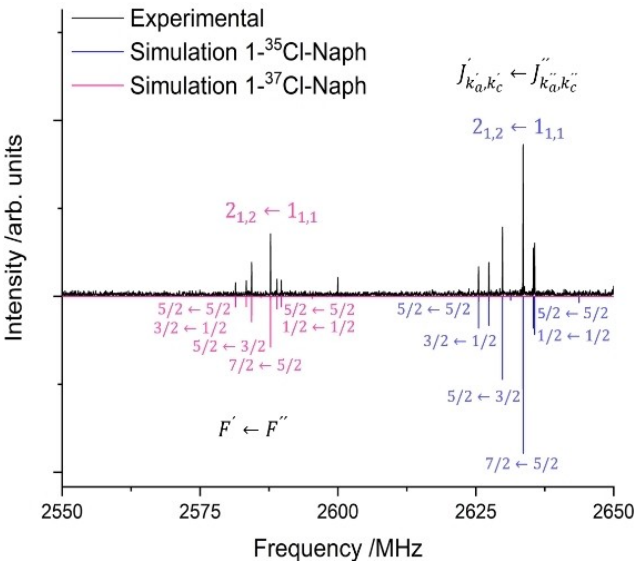

Figure 2. Excerpt of the rotational spectrum of 1-Cl-Naph. The upwards trace is the experimental spectrum, the downwards trace is a simulation of the ^{35}Cl and ^{37}Cl isotopomers, showing the hyperfine structure.

Table 1. Observed and theoretical (MP2/6-311++G(2d,p)) parameters for 1-Cl-Naph.

Parameters[a]	1–^{35}Cl-Naph	1–^{37}Cl-Naph	Theoretical
A/MHz	1526.016590(90)[b]	1514.03821(11)	1524.7
B/MHz	915.384810(66)	896.760140(87)	912.9
C/MHz	572.261814(61)	563.275690(53)	571.0
D_J/kHz	0.0125(10)	0.0158(10)	–
D_{JK}/kHz	−0.0144(22)	−0.0190(28)	–
D_K/kHz	0.0504(52)	0.0740(75)	–
d_1/kHz	−0.00556(38)	−0.00840(53)	–
d_2/kHz	−0.00082(12)	−0.00083(16)	–
$1.5\chi_{aa}$/MHz	−21.2918(18)	−19.9303(22)	−22.1
$0.25(\chi_{bb}-\chi_{cc})$	−12.64573(52)	−9.44200(61)	−11.6
χ_{ab}/MHz	54.686(54)	43.200(69)	52.1
N	555	351	–
σ/kHz	2.9	2.4	–
$\lvert\mu_a\rvert$/D	Yes	Yes	−1.3
$\lvert\mu_b\rvert$/D	Yes	Yes	1.0
$\lvert\mu_c\rvert$/D	No	No	0.0
Derived			
P_a/uÅ^2	552.02250(8)	563.49003(8)	553.6
P_b/uÅ^2	331.10317(8)	333.72444(8)	331.5
P_c/uÅ^2	0.07219(8)	0.07103(8)	0.0
χ_{aa}/MHz	−14.1945(12)	−13.2868(14)	−14.7
χ_{bb}/MHz	−18.1941(16)	−12.2405(19)	−15.8
χ_{cc}/MHz	32.3887(16)	25.5274(19)	30.6
χ_{zz}/MHz	−70.916(55)	−55.967(71)	−67.4
χ_{xx}/MHz	38.528(55)	30.440(71)	36.8
χ_{yy}/MHz	32.3887(16)	25.5274(19)	30.6
θ	46.047(2)	44.653(2)	45.3
∠C–Cl-a /°	47(2)[c]		46.6
η	−0.08657(74)	−0.0878(12)	−0.092

[a] A, B, and C are the rotational constants. D_J, D_{JK}, D_K, d_1, and d_2 are the quartic centrifugal distortion constants. χ_{aa}, χ_{bb}, χ_{cc}, and χ_{ab} are the nuclear quadrupole coupling constants from the fit in the principal inertial axis system representation. N is the number of quadrupole hyperfine components fitted. σ is the rms deviation of the fit. μ_α ($\alpha = a$, b or c) are the electric dipole moment components, Yes or No indicate if a- b- or c-type transitions have been observed. P_α ($\alpha = a$, b or c) are the planar moments of inertia, these are derived from the moments of inertia I_α as for example $P_c = (I_a + I_b - I_c)/2$. χ_{xx}, χ_{yy}, χ_{zz}, are the nuclear quadrupole coupling constants in the principal quadrupole coupling axis system obtained by diagonalization of the quadrupole coupling tensor. θ is the angle between the a and z axes. ∠C–Cl-a is the angle of the Cl–C bond with the a axis calculated from the $r_m^{(1)}$ and theoretical structures. $\eta = (\chi_{xx}-\chi_{yy})/\chi_{zz}$ is the nuclear quadrupole asymmetry parameter. [b] Standard errors in parentheses in units of the last digit. [c] Since the molecule is planar the c axis is parallel to the y axis, so diagonalization of the experimental tensor is equivalent to a rotation of an angle θ around the c axis.

Experimental Structure of 1-Cl-Naph

As expected, 1-Cl-Naph is a planar molecule as confirmed experimentally by the small value of P_c (Table 1), and the lack of μ_c dipole moment. For the rest of the structure discussion, the molecule will be treated as effectively planar with the atoms laying in the *ab* inertial plane (Figure S2). We determined the experimental structure of 1-Cl-Naph employing different methods thanks to the observation of all the heavy atom isotopologues. The first methodology, the substitution structure (r_s), is based on solving the Kraitchmann[34,35] equations to obtain atomic coordinates in the molecular frame. The Kraitchman method assumes that the bond lengths do not change upon isotopic substitution. The Kraitchman equations were solved using the KRA software (Table S2) available at the PROSPE webpage.[36] The bond distances and angles were obtained from the atomic coordinates using the EVAL tool (Table S3). An alternative is to determine the effective structure[37] (r_0). It is obtained by performing a least-squares fit of critical bond lengths, bond angles and dihedral angles to reproduce the moments of inertia of the molecule in the vibrational ground state. The r_0 structure can be improved by including correcting parameters accounting for molecular vibrations, leading to the mass-dependent structure,[38] $r_m^{(1)}$. For both the r_0 and $r_m^{(1)}$ structures the C–H bond distances were kept fixed to the theoretical values, and the experimental structures were obtained by floating certain bond distances and angles (Table S4) using the STRFIT software.[39] The rest of the parameters were derived from the atomic coordinates using EVAL. Table 2 presents the bond distances obtained with the r_s, r_0, and $r_m^{(1)}$ methods for 1-Cl-Naph compared with the theoretical structure, r_e, given by quantum-chemical computations (Table 2), and with the X-ray diffraction results.[19] The complete results for all the methods are collected in Tables S2–S3. It is noteworthy to highlight the excellent agreement between all methods, except for the r_s values concerning C_1, which, owing to its proximity to the a axis, leads to an

Table 2. Comparison of the experimental and theoretical (MP2/6-311++G(2d,p)) bond distances for 1-Cl-Naph. Atom labelling in Figure 1. The partial X-ray data correspond to liquid phase.

	X-ray[17]	r_s	r_0	$r_m^{(1)}$	r_e
C_1-C_2/Å	1.36	–	1.37(8)	1.38(1)	1.378
C_2-C_3/Å	1.41	1.415(2)	1.41(2)	1.410(4)	1.411
C_3-C_4/Å	–	1.367(3)	1.39(4)	1.387(6)	1.378
C_4-C_{10}/Å	–	1.425(2)	1.42(3)	1.421(5)	1.416
C_5-C_{10}/Å	–	1.424(1)	1.42(2)	1.422(4)	1.417
C_5-C_6/Å	–	1.367(3)	1.38(4)	1.376(7)	1.378
C_6-C_7/Å	–	1.425(2)	1.42(2)	1.422(4)	1.412
C_7-C_8/Å	–	1.382(3)	1.37(3)	1.375(5)	1.380
C_8-C_9/Å	–	1.47(1)	1.43(6)	1.43(1)	1.416
C_9-C_{10}/Å	–	1.49(2)	1.41(3)	1.41(1)	1.435
C_1-C_9/Å	1.42	–	1.41(5)	1.414(6)	1.419
C_1-Cl/Å	1.71	–	1.74(6)	1.74(1)	1.748

imaginary value, a drawback of the substitution method. The $r_m^{(1)}$ structure is presented in an overlay with the theoretical one in Figure 3.

It is interesting to compare 1-Cl-Naph, not only with the theoretical geometry, but also with the geometry of similar compounds. The first idea would be to contrast the bond lengths and angles with those of naphthalene; however, naphthalene has no permanent dipole moment, and thus it cannot be studied by microwave spectroscopy. For that reason, we compared 1-Cl-Naph with the solid-state X-ray crystallography structure of naphthalene (Figure S3).[40,41] Due to the high symmetry of naphthalene, it can be described with only four C–C bonds, and three angles (Figures S1 and S3). As explained before, there are several resonance forms arising from the π-electron delocalization (Figure S4), which determine the bond lengths. Due to this, the C_1-C_2 distance (equivalent to C_3-C_4, C_5-C_6, and C_7-C_8), has more double bond character than C_1-C_9, C_2-C_3, and C_9-C_{10}. In 1-Cl-Naph, the chlorine nucleus alters the naphthalene structure by the induction (−I) and mesomeric (+M) effects, distorting the nearby C–C bonds and angles. The most noticeable outcome is a subtle shortening of the C_1-C_9 bonds, and an opening of the C_9-C_1-C_2 angle compared to naphthalene. Those distortions are magnified in the chemical structures of Figure S3 for a better visualization.

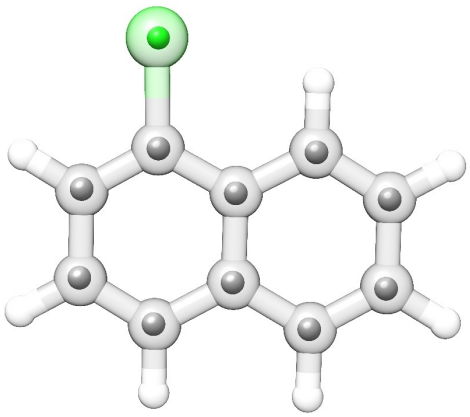

Figure 3. Overlay of the $r_m^{(1)}$ structure of 1-Cl-Naph (inner solid spheres) with the r_e structure (outer semi-transparent balls and sticks model).

A similar opening of the C-C-C angle centered at the carbon bonded to chlorine atom also happens in the smaller analogue, 1-chlorobenzene (Figure S3), studied by microwave spectroscopy.[42,43]

To analyze in depth the −I and +M effects of chlorine over naphthalene would require to study the experimental structure of the other isomer, 2-Cl-Naph, or other PCNs. Accurate rotational constants and nuclear quadrupole coupling constants for 2-Cl-Naph have been described.[16,17] However, the r_s, r_0, or $r_m^{(1)}$ structures for this molecule have not been derived. The subtle balance on the structure due to the -I and +M effects could be also characterized by exploring other halogenated naphthalenes. There has been an intense work around fluoronaphthalene, with several studies reporting precise molecular structures .[18,44,45] However, as in the case of 2-Cl-Naph, its experimental structure remains elusive, constraining the available information of bond distances and angles to theoretical values. In the case of bromonapththalene it has been much less investigated, leaving the door open for future studies.

The quadrupole coupling tensor χ^{abc} of ^{35}Cl and ^{37}Cl atoms has been determined from the fitting of the hyperfine structure of 1-Cl-Naph. Since the molecular plane is coincident with the *ab* inertial plane, the quadrupole coupling tensor has only a non-zero off-diagonal element, χ_{ab}. The *c* inertial axis is parallel to one of the quadrupole principal axis, let's say *y*. According to this, the quadrupole coupling constant χ_{cc} can be identified with χ_{yy} and the diagonalization of the χ^{abc} tensor to obtain the χ^{xyz} tensor in the principal quadrupole coupling axes is equivalent to a rotation of an angle θ around the *c* inertial axis. The results of this diagonalization are given in Table 1 and Table 3. The diagonal quadrupole coupling tensor element, $\chi_{yy}=\chi_{cc}$, directly determined from the analysis of the rotational spectrum, can be taken to calculate the ratio $\chi_{yy}(^{35}Cl)/\chi_{yy}(^{37}Cl)=1.26878(16)$ which is in excellent agreement with the best value

Table 3. Experimental rotational constants and nuclear quadrupole coupling constants for 1-Cl-Naph, 2-Cl-Naph, and chlorobenzene.

	1-Cl-Naph		2-Cl-Naph[a]		Chlorobenzene[b]	
Parameters[c]	^{35}Cl	^{37}Cl	^{35}Cl	^{37}Cl	^{35}Cl	^{37}Cl
A/MHz	1526.016590(90)[d]	1514.03821(11)	2731.9361(1)	2727.1325(1)	5672.27687(16)	5672.27476(82)
B/MHz	915.384810(66)	896.760140(87)	581.67545(3)	567.56056(6)	1576.786667(18)	1532.788685(34)
C/MHz	572.261814(61)	563.275690(53)	479.65182(3)	469.870(6)	1233.675023(18)	1206.574989(33)
χ_{zz}/MHz	−70.916(55)	−55.967(71)	−71.198(5)	−56.095(8)	−71.2359(11)	−56.1445(16)
χ_{xx}/MHz	38.528(55)	30.440(71)	38.318(5)	30.18	38.21533(57)	30.1200(27)
χ_{yy}/MHz	32.3887(16)	25.5274(19)	32.880	25.91	32.0205(16)	26.0244(27)
η	−0.08657(74)	−0.0878(12)	−0.07638(5)	−0.0761(3)	−0.072924(11)	−0.072925(90)
$\chi_{yy}(^{35}Cl)/\chi_{yy}(^{37}Cl)$[e]	1.26878(16)		1.2692		1.23040(14)	

[a] From reference 16. [b] From reference 47. [c] *A*, *B*, and *C* are the rotational constants. χ_{xx}, χ_{yy}, χ_{zz}, are the nuclear quadrupole coupling constants in the principal quadrupole coupling axis system obtained by diagonalization of the quadrupole coupling tensor. $\eta=(\chi_{xx}-\chi_{yy})/\chi_{zz}$ is the nuclear quadrupole asymmetry parameter. [d] Standard errors in parentheses in units of the last digit. [e] The quadrupole moments ratio for $Q(^{35}Cl)/Q(^{37}Cl)$ is 1.26889(3).[46]

of the quadrupole moments ratio, $Q(^{35}Cl)/Q(^{37}Cl) = 1.26889(3)$.[46] The angle $\theta = 46.047(2)^\circ$ is calculated from the diagonalization of the quadrupole coupling tensor as the angle between the *a* inertial axis and the quadrupole coupling axis *z*. In molecules with a single Cl–C bond the asymmetry parameter $\eta = \frac{(\chi_{xx}-\chi_{yy})}{\chi_{zz}}$ gives a measure of the deviation of the χ^{xyz} tensor from the cylindrical symmetry around the *z* axis. This axis is usually coincident with the Cl–C bond as occurs for 1-Cl-Naph for which the angle formed by this bond with the *a* inertial axis has been calculated from the $r_m^{(1)}$ structure to be 47(2)° (see Table 1), in excellent agreement with the diagonalization θ value.

The values of the quadrupole coupling constants obtained for 1-Cl-Naph are comparable to those reported for 2-Cl-Naph,[16] and for chlorobenzene[47] (Table 3). In the three cases η has a low value that indicates a small degree of π bonding character showing an excess of n_y electron density with respect to n_x. This excess seems to be slightly higher in 1-Cl-Naph with respect to 2-Cl-Naph and chlorobenzene.

Conclusions

We analyzed the gas-phase structure of 1-chloronaphthalene by chirped-pulse Fourier transform microwave spectroscopy coupled with supersonic expansion. The experimental spectrum featured a hyperfine structure arising from the nuclear quadrupole coupling of the ^{35}Cl and ^{37}Cl nucleus. A single conformer was predicted by theoretical computations guiding a straightforward assignment. We detected all the heavy atoms isotopologues, which allowed us determining a precise experimental structure for 1-Cl-Naph following different approaches. All the experimental structures are consistent with a C–C bond lengths shortening together with the opening of the C–C–C angle, relative to pure naphthalene. The comparison of our data and the data obtained with other techniques, such as rotationally resolved high-resolution electronic spectroscopy, can provide important information about the properties of PCNs. Our work sets the basis for future microsolvation studies of 1-Cl-Naph and provides precise parameters for the search of this molecule in the ISM.

Author Contributions

Pablo Pinacho: formal analysis, writing – original draft, writing – review & editing. Pablo Gómez: investigation, formal analysis. Juan Carlos López: conceptualization, funding acquisition, project administration, investigation, formal analysis, writing – review & editing. Susana Blanco: conceptualization, funding acquisition, project administration, investigation, formal analysis, writing – review & editing.

Acknowledgements

S. B., J. C. L., and P. P. acknowledge the Ministerio de Ciencia e Innovacion (Grant PID2021-125207NB-C33), the Ministerio de Economía y Competitividad (Grant CTQ2016-75253-P) and Junta de Castilla y León (Grant INFRARED-FEDER IR2020-1-UVa02) for financial support. P.P. acknowledges a Maria Zambrano grant (UPV/EHU, Ministry of Universities, Recovery, Transformation, and Resilience Plan – Funded by the European Union – Next Generation EU, MAZAM22/16)

Conflict of Interests

Authors declare no conflict of interest.

Data Availability Statement

The data that support the findings of this study are available in the supplementary material of this article.

Keywords: Microwave spectroscopy · Structure elucidation · Polychlorinated naphthalenes (PCNs) · Jet cooled molecules · Pollutant

[1] A. G. G. M. Tielens, *Annu. Rev. Astron. Astrophys.* **2008**, *46*, 289–337.
[2] F. Jesus, J. L. Pereira, I. Campos, M. Santos, A. Ré, K. Keizer, A. Nogueira, F. J. M. Gonçalves, N. Abrantes, D. Serpa, *Sci. Total Environ.* **2022**, *820*, 153282.
[3] D. S. N. Parker, F. Zhang, Y. S. Kim, R. I. Kaiser, A. Landera, V. V. Kislov, A. M. Mebel, A. G. G. M. Tielens, *Proc. Nat. Acad. Sci.* **2012**, *109*, 53–58.
[4] IUPAC. Compendium of Chemical Terminology, the Gold Book, 2nd ed. Compiled by A. D. McNaught and A. Wilkinson. Blackwell Scientific Publications, Oxford, **1997**. https://doi.org/10.1351/goldbook.
[5] G. Liu, Z. Cai, M. Zheng, *Chemosphere* **2014**, *94*, 1–12.
[6] N. Yamahista, K. Kannan, T. Imagawa, A. Miyazaki, J. P. Giesy, *Environ. Sci. Technol.* **2000**, *34*, 4236–4241.
[7] Q. Kang, S. Bao, B. Chen, *J. Hazard. Mater.* **2021**, *409*, 124895.
[8] K. Sankoda, K. Nomiyama, T. Yonehara, T. Kuribayashi, R. Shinohara, *Chemosphere* **2012**, *88*, 542–547.
[9] A. K. Lemmens, D. B. Rap, J. M. M. Thunnissen, B. Willemsem, A. M. Rijs, *Nat. Commun.* **2020**, *11*, 269.
[10] B. A. McGuire, R. A. Loomis, A. M. Burkhardt, K. L. K. Lee, C. N. Shingledecker, S. B. Charnley, I. R. Cooke, M. A. Cordiner, E. Herbst, S. Kalenskii, M. A. Siebert, E. R. Willis, C. Xue, A. J. Remijan, M. C. McCarthy, *Science* **2021**, *371*, 1265–1269.
[11] B. A. McGuire, *Astrophys. J. Suppl. Ser.* **2021**, *259*.
[12] S. Jansson, J. Fick, S. Marklund, *Chemosphere* **2008**, *72*, 1138–1144.
[13] W. Smulek, A. Zdarta, A. Pacholak, T. Runka, E. Kaczorek, *Ecotoxicol. Environ. Saf.* **2019**, *185*, 109707.
[14] M. Fujita, T. Ishizuya, T. Hikida, Y. Mori, *Chem. Phys.* **1989**, *139*, 261–264.
[15] T. Troxler, B. A. Pryor, M. R. Topp, *Chem. Phys. Lett.* **1997**, *274*, 71–78.
[16] D. F. Plusquellic, S. R. Davis, F. Jahanmir, *J. Chem. Phys.* **2001**, *115*, 225–235.
[17] R. A. Singh, S. N. Thakur, *Mol. Phys.* **1978**, *36*, 1053–1059.
[18] R. A. Singh, S. N. Thakur, *J. Mol. Spectrosc.* **1983**, *102*, 1–12.
[19] H. Drozdowski, *J. Mol. Struct.* **2020**, *526*, 391–397.
[20] G. G Brown, B. C. Dian, K. O. Douglass, S. M. Geyer, B. H. Pate, *J. Mol. Spectrosc.* **2006**, *238*, 200–212.
[21] J. C. López, A. Macario, A. Verde, A. Pérez-Encabo, S. Blanco, *Molecules* **2021**, *26*, 7585.
[22] S. Blanco, A. Macario, J. C. López, *Phys. Chem. Chem. Phys.* **2021**, *23*, 13705–13713.
[23] a) C. Lee, W. Yang, R. G. Parr, *Phys. Rev. B* **1988**, *37*, 785–789; b) A. D. Becke, *J. Chem. Phys.* **1993**, *98*, 5648–5652.

[24] M. J. Frisch, J. A. Pople, J. S. Binkley, *J. Chem. Phys.* **1984**, *80*, 3265–3269.
[25] S. Grimme, J. Antony, S. Ehrlich, H. J. Krieg, *Chem. Phys.* **2010**, *132*, 154101.
[26] A. D. Becke, E. R. Johnson, *J. Chem. Phys.* **2005**, *122*, 154101.
[27] C. Møller, M. S. Plesset, *Phys. Rev.* **1934**, *46*, 618–622.
[28] Gaussian 16, Revision A.03, M. J. Frisch, et al., *Gaussian*, *Inc.*, *Wallingford CT*, **2016**.
[29] D. Plusquellic, JB95, available at http://www.nist.gov/pml/electromagnetics/grp05/jb95.cfm.
[30] W. Gordy, R. L. Cook, *Microwave molecular spectra*, Wiley-Interscience, New York **1972**, vol. 11.
[31] J. K. G. Watson, in *Vibrational Spectra and Structure a Series of Advances, Vol 6* ed. J. R. Durig, Elsevier, New York **1977**, pp. 1–89.
[32] H. M. Pickett, *J. Mol. Spectrosc.* **1991**, *148*, 371–377.
[33] Z. Kisiel, L. Pszczolkowski, I. R. Medvedev, M. Winnewisser, F. C. De Lucia, E. Herbst, *J. Mol. Spectrosc.* **2005**, *233*, 231–243.
[34] J. Kraitchman, *Am. J. Phys.* **1953**, *21*, 17–24.
[35] C. C. Costain, *Trans. Am. Crystallogr. Assoc.* **1966**, *2*, 157–164.
[36] PROSPE – Programs for ROtational SPEctroscopy, http://www.ifpan.edu.pl/~kisiel/prospe.htm, (accessed February, 2024).
[37] H. D. Rudolph, *Struct. Chem.* **1991**, *2*, 581–588.
[38] J. K. G. Watson, A. Roytburg, W. Ulrich, *J. Mol. Spectrosc.* **1999**, *196*, 102–119.
[39] Z. Kisiel, *J. Mol. Spectrosc.* **2003**, *218*, 58–67.
[40] D. W. J. Cruickshank, *Acta Crystallogr.* **1957**, *10*, 504–508.
[41] D. W. J. Cruickshank, R. A. Sparks, *Proc. R. Soc. London Ser. A* **1960**, *258*, 270–285.
[42] G. Roussy, F. Michel, *J. Mol. Struct.* **1976**, *30*, 399–407.
[43] S. Cradock, J. M. Muir, D. W. H. Rankin, *J. Mol. Struct.* **1990**, *220*, 205–215.
[44] W. Majewski, D. F. Plusquellic, D. W. Pratt, *J. Chem. Phys.* **1989**, *90*, 1362–1367.
[45] S. J. Carey, M. Sun, S. G. Kukolich, *J. Mol. Spectrosc.* **2014**, *304*, 25–27.
[46] A. C. Legon, J. Thorn, *Chem. Phys. Lett.* **1993**, *215*, 554–560.
[47] P. M. Dorman, B. J. Esselman, P. B. Changala, M. C. McCarthy, R. C. Woods, R. J. McMahon, *J. Mol. Spectrosc.* **2023**, *394*, 111776.

Manuscript received: January 25, 2024
Revised manuscript received: February 23, 2024
Accepted manuscript online: March 12, 2024
Version of record online: April 8, 2024